JGISE Vol. 8 No. 1 (2025), pp. 66 - 73 | https://doi.org/10.22146/jgise.98778

JGISE
Journal of Geospatial Information Science and Engineering
ISSN: 2623-1182 | https://jurnal.ugm.ac.id/jgise

Semi-Automatic 3D Modeling of Rooftop Types from Aerial Photos

Arsa Fa'iz Nursyahrial, Hanif Ilmawan

Department of Earth Technology, Vocational College, Universitas Gadjah Mada, Indonesia

Correspondent Author: Hanif Ilmawan **| Email:** hanif.ilmawan@ugm.ac.id

Received: 30/07/2024 Revised: 31/05/2025 Accepted: 15/06/2025

ABSTRACT

Urban planning has dynamic problem as time goes by. 3D City Model is one of solutions to help planners in decision making, because it can represent real objects in high detail, including the rooftop type. In this research, case study of 3D City Model located in the office area of Wonogiri Regency Government, which was processed from aerial photos using semi-automatic method with LoD 2 standart. This semi-automatic method used Computer Generated Architecture (CGA) rules that contained commands to create objects based on their input. The result was a 3D model of the building along with road and landscape. The roof shape of 3D building model was compared to aerial photos in order to evaluate the visual accuracy, specifically aiming for completeness, correctness, and accuracy values above 85%. The result showed that the flat and shed have the highest accuracy, while the gable roof has low accuracy, though they were all above 85% accuracy. This means that the semi-automatic method has potential for 3D modeling purpose in any kind of standard roof types.

Keywords: 3D City, photogrammetry, nDSM, urban planning, Computer Generated Architecture

1. Introduction

Urban planning is one of the regional planning aspects and serves to plan an area using spatial data with the aim of making each space function effectively and supporting the survival of the people who live (Raven et al., 2018). This space planning activity needs to be carried out in all areas, both cities and villages in detail in the form of a combination of building forms and objects contained in the area so that the function of space can be more optimal and attractive (Udoh et al., 2020).

As time goes by, the problems in urban planning are increasingly dynamic and diverse, so detailed and dynamic data representations are needed so that they can be analyzed in more depth. Regency/city governments in Indonesia have already prepared spatial planning data, but it is still in the form of 2D maps that are realized in the Rencana Tata Ruang Wilayah (RTRW)/ Regional Spatial Plan and Rencana Detil Tata Ruang (RDTR)/ Detailed Spatial Plan. The solution to overcome this problem is to use a 3D City Model. This is because 3D models can represent data better than 2D map models (Biljecki et al., 2015; Herbert & Chen, 2015; Uggla et al., 2023; Willenborg et al., 2018). In addition, the 3D City Model can also be updated dynamically as problems change over time (Bieda et al., 2020; Trikusuma et al., 2021).

One of the most widely used concepts in 3D urban modeling is the level of detail (LoD) (Biljecki, 2017). The concept of LoD refers to the degree of information and geometric complexity included in a 3D model. It determines how much detail is represented in the visual and structural components of the model. At the most basic level, LoD 1 provides simple representations of buildings, typically shown as block models with flat roofs. These models lack detailed features but are sufficient for certain types of analysis. As the level increases to LoD 2, LoD 3, and LoD 4, the models become progressively more detailed. At these higher levels, roof structures begin to reflect the actual shapes and features of real buildings. This gradual increase in detail allows for more realistic and functionally rich 3D representations, which are useful in various urban planning and architectural applications.

In spatial planning applications, 3D models often utilize the LoD 2 concept due to its relatively simple structure while still providing a more realistic representation through the inclusion of roof geometry. The presence of roof elements in the model allows for analyses such as the estimation of solar energy potential in urban planning contexts (Peters et al., 2022). However, practical implementation of roof modeling requires special attention,

as roof shapes are highly diverse and often difficult to interpret accurately through digital interpretation.

In this research, the creation of a 3D City Model for urban planning takes a case study in the office area of the Wonogiri Regency Government. This is because based on the Central Java RTRW 2009-2029, the area is projected to become a new economic strategic area in the Greater Solo, Central Java. This 3D City Model creation method can use automatic (Danilina et al., 2018; Pađen et al., 2022) and semi-automatic (Badwi et al., 2022; Buyukdemircioglu et al., 2018) methods. The automatic method means that the software used to create has already defined the syntax, attribute grammar, and object parameters, while in the semi-automatic methods the parameters are defined manually (Firdaus et al., 2020). Each of these methods has advantages and disadvantages. The automatic method has the advantage of fast and efficient modeling time, but it is difficult to model models that have a high level of accuracy. In semi-automatic methods, the advantages are generally the same as automatic methods, but can represent objects better. One of the modeling techniques with this method is Computer Generated Architecture (CGA), which is a programming grammar that contains a rule or rule that contains object parameters to be modeled (Kelly, 2021). The weakness of this semi-automatic method is that for modeling objects that have a high level of accuracy, the rules needed will be more complicated, so this method is suitable for use at a low LoD.

In the process of making this 3D City Model, the Level of Detail chosen is LoD 2, so the method used is semi-automatic, because it can quickly and effectively model an object. The constituent data used in making this 3D City Model is aerial photography data of Wonogiri Government office area, which is then processed into a Digital Terrain Model (DTM) and Digital Surface Model (DSM) to extract object heights using the Normalized Digital Surface Model (nDSM) algorithm. In addition, aerial photographs are also used for the extraction of building footprints that will be created in 3D using semi-automatic methods.

The result of 3D City creation is a 3D model of the building. The 3D shape of the building is differentiated based on the shape of the roof due to the different level of complexity of the building roof. Visual accuracy test is conducted using completeness, correctness, and accuracy parameters to determine the quality of the resulting 3D City model. The results of this research can show the accuracy level of the suitability of the 3D City model based on the complexity of the roof type of the building modeled using the semi-automatic method. In the future, the accuracy results of the 3D model of each type of building roof are expected to further optimize the creation of 3D City Models with semi-automatic methods that are fast and effective, and can help overcome urban planning problems that always change over time.

2. Methods

The research area is in Wonogiri Regency, Central Java, specifically in the regency government office area, Giripurwo, Wonogiri District.

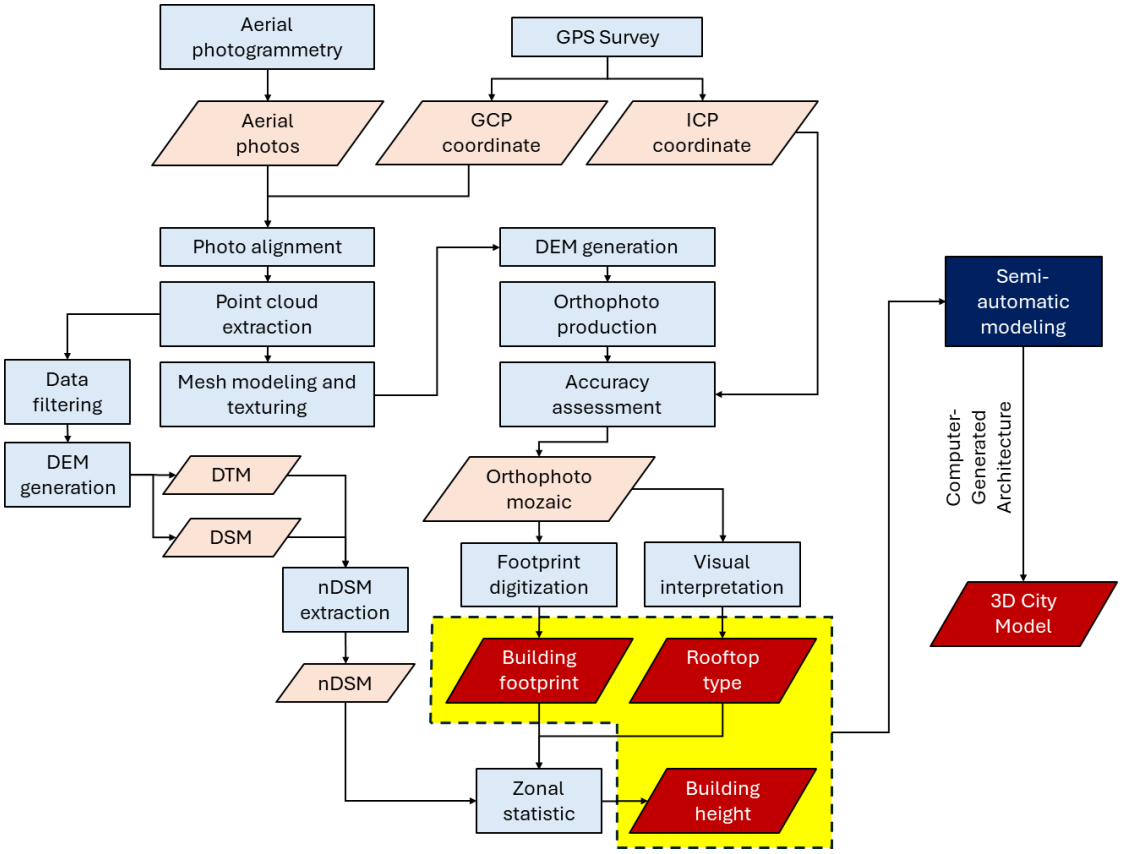

Figure 2 Workflow of 3D city modeling

The data used to create the 3D City Model is aerial photo data that captured that area, with a total of 1,243 aerial photos taken in January 2023 and has 5 Independent Control Point (ICP) as geometric accuracy assessment as shown in Table 1. The flight altitude of the UAV is 360 m, with a ground resolution of 3.96 cm/pixel. The whole process for 3D city modeling is shown in Figure 2. The map of the research area is shown in Figure 3, bordered with red line.

Table 1 Measured ICP

Points	X (m)	Y (m)	Z (m)
CWNG001	491807.5737	9136249.5576	159.9147
CWNG002	492463.0344	9136474.8400	157.1404
CWNG003	493728.2765	9136571.3452	179.5095
CWNG004	493209.1563	9137307.3061	154.7872
CWNG005	491777.5791	9135589.1289	162.4414

2.1. Aerial Photo Processing

The 1,243 aerial photos were processed using Agisoft Metashape software. The first step is to align the photos, this process serves to adjust the orientation of each photo and look for similar features/objects in each photo so that they can be bound to each other. The result of aligned photo processing is sparse clouds data. The next step is to make dense clouds. Dense cloud is a collection of point clouds data arranged to form an object on aerial photos. This dense clouds data will be used as the basic data for making DTM and DSM.

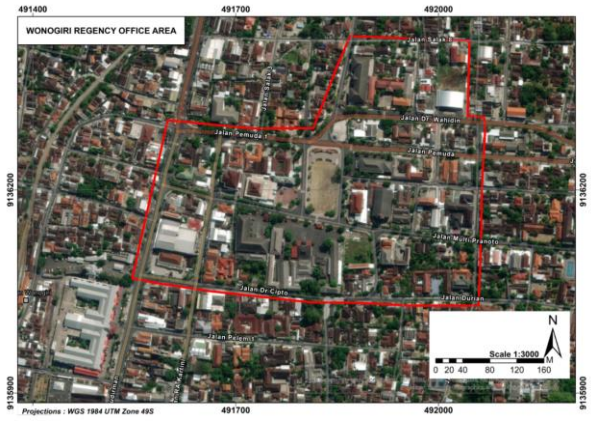

Figure 2 Map of research area

The next processing is mesh creation and texture creation. This mesh creation serves to reconstruct the object into 3D from the shape and position of the aerial photo viewpoint. The concept of making 3D uses the principle of interpolation from dense clouds data in the form of point clouds. After 3D is formed, texture creation is carried out which functions to adjust the quality of the lighting hue and flatten the texture of the processed aerial photo data to make it smoother.

The last step of processing this aerial photo is making DEM and orthophoto. DEM data is made from dense clouds, the data resulting from making this DEM is still in the form of DSM because it has not been filtered. In addition, the resulting DEM data is also used as surface data for making orthophoto. The projection system used in the making of orthophoto and DEM is set to UTM Zone 49S WGS 1984.

The results of the orthophoto that has been made need to be tested for geometric accuracy to determine the quality of aerial photography coordinates against actual field coordinates, both vertically and horizontally [8]. The formulas of this geometric accuracy test are presented in equation $CE90 = C_{CE} \times RMSE_h$ (1) and $LE90 = C_{LE} \times RMSE_v$ (2).

$$CE90 = C_{CE} \times RMSE_h \quad (1)$$

$$LE90 = C_{LE} \times RMSE_v \quad (2)$$

where,

$RMSE_h$: horizontal root mean square error of aerial photo
$RMSE_v$: vertical root mean square error of aerial photo
C_{CE} : circular error constant (1.5175)
C_{LE} : linear error constant (1.6499)

Meanwhile, RMSE calculation shown in equations $RMSE_h = \sqrt{D^2/n}$ (3), $RMSE_v = \sqrt{\sum(Z_{data} - Z_{check})^2/n}$ (4), and $D^2 = \sum|(X_{data} - X_{check})^2 + (Y_{data} - Y_{check})^2|$ (5).

$$RMSE_h = \sqrt{D^2/n} \quad (3)$$

$$RMSE_v = \sqrt{\sum(Z_{data} - Z_{check})^2/n} \quad (4)$$

$$D^2 = \sum|(X_{data} - X_{check})^2 + (Y_{data} - Y_{check})^2| \quad (5)$$

In this research, the CE90 and LE90 values are considered to pass the geometric accuracy assessment if the values are <2 m and <1 m, respectively. This refers to the level of scale accuracy used, which is at a scale of 1:5000 class 3 of the Peraturan Badan Informasi Geospasial Nomor 18 Tahun 2021. After the aerial photo has passed the geometric accuracy test, it can be cropped based on the Area of Interest (AOI) border as shown in Figure 2.

2.2. DTM, DSM, and nDSM Extraction

DSM data has been generated from the process of creating dense clouds during the processing of previous aerial photographs, so to create DTM data, filtering is required using Agisoft Metashape software to separate objects with terrain from DSM data. This DTM data will be used as the ground for the 3D City Model. The results of filtering DSM into DTM are in raster format, which both are used as material for making Normalized Digital Surface Model (nDSM) (Jang et al., 2020). nDSM is used to extract the height of building objects, the value of which is obtained from a subtraction of DSM from DTM using a raster calculator in ArcGIS Pro software. The results of making nDSM are also stored in the form of raster data.

2.3. Footprint and Building Height Extraction

Footprint data is used as surface data on each building object, which is obtained through the process of digitizing the geometric corrected orthophoto in the previous accuracy test. The result of the footprint digitization process is vector data. This data is then used to extract the height of each building object.

The height extraction stage of building objects is carried out using ArcGIS Pro software with the "Zonal Statistics as Table" tools. This tool functions to detect the statistical value of height from raster data in each zone bounded by vector data (Winsemius & Braaten, 2024). In this study, the vector data used as a boundary for height extraction calculations is footprint data from orthophoto digitization and the raster data used is nDSM data. This is because nDSM data is data that only contains raster values of objects on the ground. The result of height extraction is a data table containing information on the maximum, average and minimum height values of each building object. The height extraction table is then combined with the building footprint vector data.

Footprint data that already contains the height value of the data extraction results, then added the attribute of the type of roof shape of each building. Defining the type of roof on each building is done manually by identifying each building object one by one in the orthophoto data. In this research, there are 5 types of roofs identified, which are hip, gable, shed, pyramid, and flat.

2.4. Semi-Automatic Modeling Process

The process of making 3D City Model uses semi-automatic method. This method differs from manual approaches in which the building's shape is entirely reconstructed by humans. It also does not delegate the entire interpretation and 3D modeling process to the computer. In the semi-automatic method, the 3D modeling process is carried out by the computer with human intervention. Humans are responsible for providing input in the form of modeling parameters, such as object height and roof type, while the processing tasks are done by the computers. There is a mutually dependent division of roles between humans and computers in semi-automatic modeling as indicated in Figure 4.

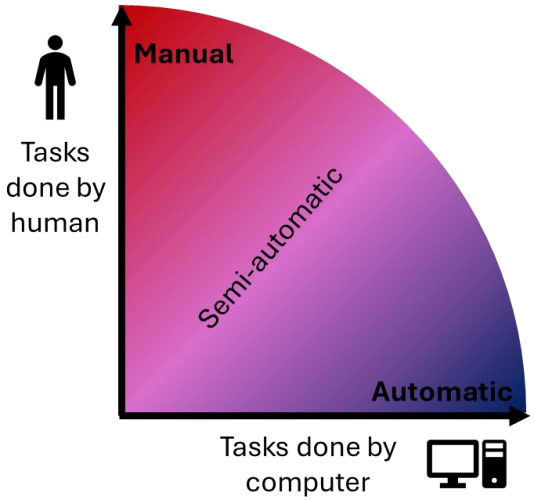

Figure 3 Human and computer contributions in different modeling methods

As shown in Figure 2, the semi-automatic modeling method requires only three essential inputs: building height, building footprint, and rooftop type. While the DTM and orthophoto are not mandatory, they remain useful for enhancing model accuracy. Both datasets are imported into CityEngine, where the DTM serves as the ground surface and the orthophoto is used as texture data. This setup simplifies the process of creating a 3D city model of the buildings. Furthermore, 3D modeling can be performed at LoD 2 using footprint data and the Computer-Generated Architecture (CGA) rule scripting in CityEngine (Badwi et al., 2022). Some of the CGA commands used to generate the basic 3D building form include defining object height and roof type. The CGA rules can automatically generate the building and roof geometry based on the building footprint. Subsequently, extrusion is applied according to the specified height, and textures such as wall and roof colors can be assigned.

In this research, the level of accuracy of the modeled object is at the LoD 2 level, where the object is modeled in the form of a block parallelogram shape and features the shape of the roof structure on each building (Biljecki, 2017). A comparison of the level of fidelity at each LoD level is presented in Figure 4.

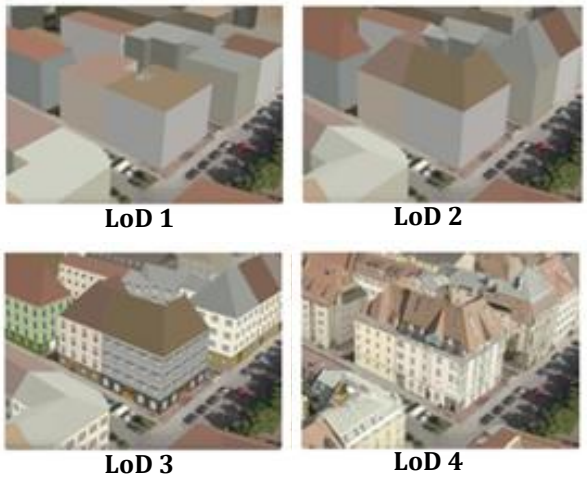

Figure 4 Visualization in each level of LoD (Biljecki, 2017)

2.5. Evaluations from Visual Accuracy Assessment

The 3D City model that has been created then needs to be tested for accuracy in order to determine the quality of the data and find out which roof types are suitable to be modeled to form 3D City with the semi-automatic method. Accuracy test used the accuracy test used is visual accuracy, which compares data from the 3D model to orthophoto data on the roof type. The parameters for determining the quality of the visual accuracy test results use completeness, correctness, and accuracy testing with an accuracy threshold of at least 85% of each of at least 30 samples taken on each roof type (Foody, 2002; Heipke et al., 1997; Zheng et al., 2017). The formulas for calculating completeness, correctness, and accuracy are presented in equations $Completeness = TP/(TP + FN)$ (6), $Correctness = TP/(TP + FP)$ (7), and $Accuracy = TP/(TP + FN + FP)$ (8).

$$Completeness = TP/(TP + FN) \quad (6)$$

$$Correctness = TP/(TP + FP) \quad (7)$$

$$Accuracy = TP/(TP + FN + FP) \quad (8)$$

where,

TP : True Positive, the number of objects that are present in both 3D city model and actual data

FP : False Positive, the number of objects that are present in the 3D model, but not in the actual data

FN : False Negative, the number of objects that are present in the actual data but not in the 3D model

The assessment is conducted by comparing the completion of the sides of each roof type against the roof data in the orthophoto. The results of the comparison are then entered into the computation of completeness, correctness, and accuracy calculations. If the total accuracy value of the samples taken has passed the 85% threshold, then the 3D City model can be accepted for its data quality. In addition, this accuracy test can also determine which roof types are good to be modeled using the semi-automatic method with CGA rules. The testing technique of this visual accuracy test is presented in Figure 5.

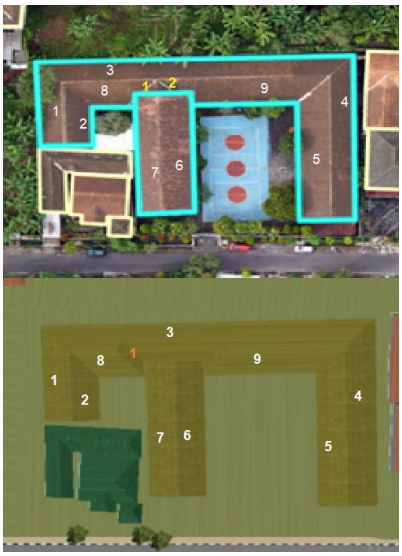

Figure 5 Visual accuracy assessment technique. White number indicated TP, yellow indicated FP, and orange indicated FN

3. Results and Discussion

3.1. Aerial Photo Processing Results

Aerial photos that have been processed from 1,243 photos produce the same Ground Sampling Distance (GSD) as the aerial photo acquisition data specifications. The results of aerial photo processing in the form of orthophoto are then tested for horizontal and vertical accuracy based on the CE90 and LE90 values. Horizontal and vertical accuracy testing is done by comparing the coordinates on the actual ICP position data to the ICP position data on aerial photographs. The test results are shown in Table 2.

Based on the Table 2, the RMSE value obtained in the horizontal accuracy test is 0.6667 and in the vertical accuracy test is 0.4381, while for the CE90 value the result is 0.1013 and the LE90 value is 0.7229. Referring to the Peraturan Kepala Badan Informasi Geospasial Tahun 2021, the calculation results meet the 1:5000 scale specification standard in class 3 with a maximum threshold of CE value of 2 m and LE of 1 m. After the orthophoto data have passed the CE and LE assessment standards, cropping of the Area of Interest (AOI) research study can then be applied to the Wonogiri Regency government office area. This is necessary so that further data processing is lighter and can focus more on the research study area only.

Table 2 Horizontal and vertical accuracy assessment results

Accuracy assessment	RMSE	CE90	LE90
Horizontal	0.6667	0.1013	-

Vertical	0.4381	-	0.7229

3.2. DTM, DSM, and nDSM Results

In processing aerial photos, there is dense clouds data generated. The data still represents the earth's surface and the objects on it or commonly called DSM data. Automatic filtering is used to make topographic data of the earth's surface only to produce DTM data. From the DTM and DSM data, nDSM data is also produced which is obtained from reducing DSM to DTM using a raster calculator, which only represents the height of objects above the earth's surface without being accompanied by surface topography data.

The range of pixel values in DTM, DSM, and nDSM raster data represents the height value of an object. In nDSM data, the range of pixel values ranges from 0 to 33.3646 only, this is because the range of values is the result of subtraction from DSM data to DTM data, so it can be determined that the height of objects in the data has a maximum height of up to 33.3646 meters. The height data from nDSM is then extracted to get the height value of each building object based on its footprint.

3.3. Footprints Extraction Results

The result of footprint extraction is to classify buildings based on their area. In this study, the area is divided into 7 areas, which are public facilities, educational institutions, residential areas, regency government offices, public offices, shops, and places of worship. Determination of the type of area is based on the results of field surveys and interpretation through aerial photos. The footprint data contains attributes that have height values and roof types. Height data is obtained from the extraction of height from nDSM data, and roof type data is obtained from visual interpretation of aerial photos. There are 5 types of roofs that have been identified, namely hip, gable, shed, flat, and pyramid.

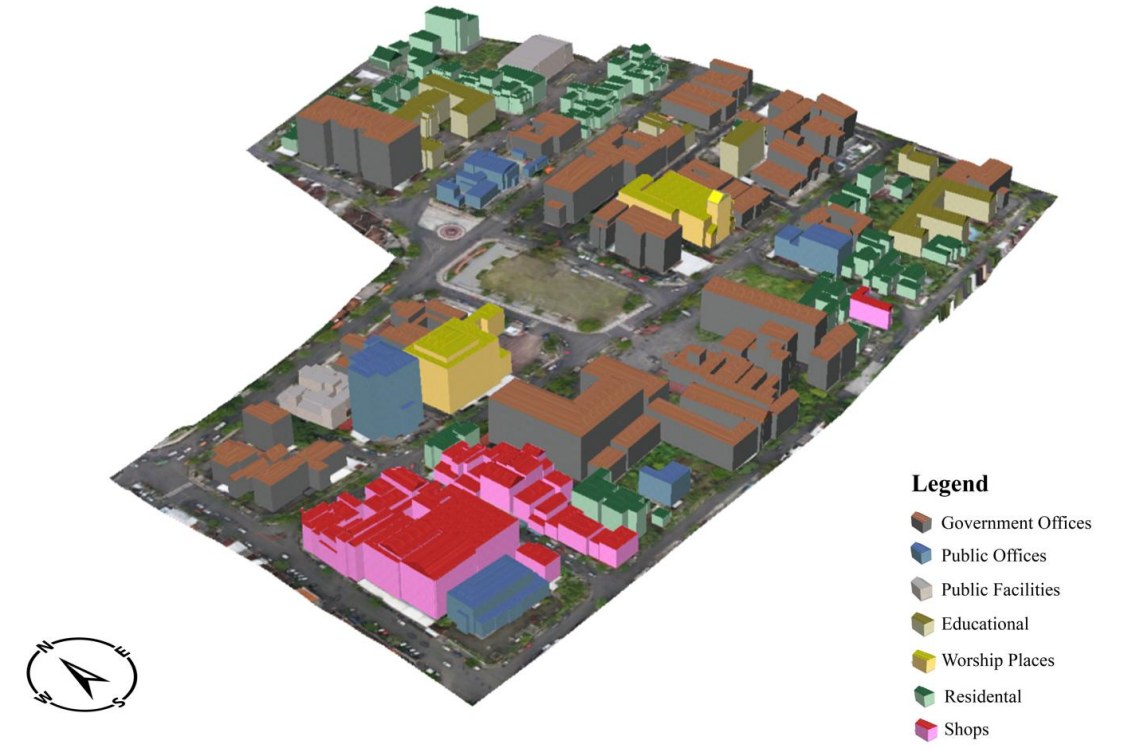

Figure 6 3D City Model of Wonogiri Government Office Area

Roof type	Hip	Gable	Shed	Pyramid	Flat
Zonal statistic value	MAX	MAX	MAX	MAX	AVERAGE
Objects in aerial photo				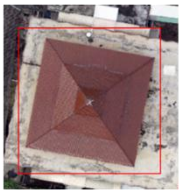	
3D model	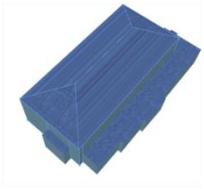	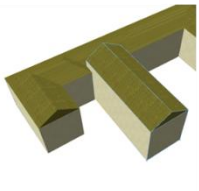	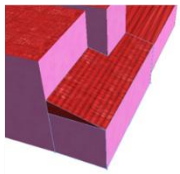	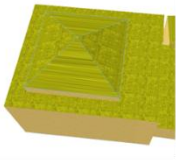	

Figure 7 3D model result of each roof type

3.4. 3D City Model Results

The footprint data that has been created and its attributes contain information on the height and roof type of each building can then be processed into a 3D City Model. The creation of 3D City Model semi-automatic method with CGA Rules using CityEngine software succeeded in modeling effectively with a total of 179 buildings. Respectively 2 buildings in public facilities, 9 buildings in educational institutions, 65 buildings in residential areas, 60 buildings in district government offices, 14 buildings in public offices, 25 buildings in residential areas, and 4 buildings in places of worship.

In terms of building height, this research analyzes the distribution of building heights based on each type of roof. This is because different roof shapes have different height references. The results of the building height distribution show that the flat roof type has an average height of 5.739 m, gable 5.990 m, hip 6.599 m, pyramid 6.142 m, and shed 4.878 m. The tallest building modeled three-dimensionally on the 3D City Model is the gable roof type with a height of 19,925 m, while the lowest is the flat roof type with a height of 2,389 m. Hip, gable, shed and pyramid roofs use the maximum height value (MAX), while flat roofs use the average height (MEAN) (Figure 7). The final result of creating a 3D City Model of the Wonogiri Regency government office area is presented in **Error! Reference source not found.** 6 with a legend classification based on the type of area.

3.5. Evaluations from Visual Accuracy Assessment Results

The results of the 3D City Model that has been made are then tested visually on the building to determine the quality of 3D data and the effectiveness of the semi-automatic CGA rules method in modeling each type of roof. This visual accuracy testing technique uses 30 samples of each roof type, then calculated using the completeness, correctness, and accuracy parameters. The results of the visual accuracy test are presented in Table 3 Visual accuracy assessment result
based on roof typesbelow.

Table 3 Visual accuracy assessment result based on roof types

Roof type	Completeness (%)	Correctness (%)	Accuracy (%)
Hip	99.63	94.03	93.83
Gable	96.28	89.63	86,41
Flat	100	100	100
Shed	100	100	100
Pyramid	93.47	93.65	88.84

Based on Figure 7, the accuracy value for all roof types is above 85%, which means it passed the threshold. The highest level of accuracy is found in buildings with flat and shed roof types with a value of 100%, which means there are no errors at all. The gable and pyramid roof types have the lowest accuracy level and are almost close to the 85% tolerance threshold, with values of 86.41% and 88.84% respectively. The cause of some of these discrepancies or errors is due to the low level of LoD used, causing differences in the shape of the roof of the building object in the 3D model to the original roof model, which results in some parts of the original building roof that are not modeled in the 3D model. Another cause is that the CGA

rules algorithm sometimes detects the shape of the footprint as a complex object, so that the generated model can create new parts on the roof of the building where these parts are not found on the original object. The accuracy test results for each roof type show that 3D building modeling using CGA rules for LoD 2 level has high accuracy for buildings with flat, shed, and hip roof types, and less than maximum accuracy for modeling buildings with gable and pyramid roof types.

4. Conclusion

Aerial photos of the Wonogiri Regency Government Office Area that have been processed with Circular Error (CE90) accuracy of 0.1013 m and Linear Error (LE90) of 0.7229 m can be used as basic data to create and produce a 3D City Model of the Wonogiri Regency Government Office Area using the semi-automatic method with CGA rules and LoD 2 accuracy level. The visual accuracy test conducted on the 3D City Model data is also acceptable in quality which has a value above the 85% threshold based on sampling of each roof type. However, when described based on the quality of modeling by roof type, flat, shed, and hip roofs have high accuracy when modeled using the semi-automatic CGA rules method, while gables and pyramids have low accuracy. This is influenced by the low LoD level used as well. In the upcoming research, the results of this semi-automatic roof type making visual quality assessment can be used for further analysis and development in making 3D City Model with a higher LoD level in order to help solve urban planning problems.

5. Conflict of Interest

The authors declare no competing interest.

6. References

Badwi, I. M., Ellaithy, H. M., & Youssef, H. E. (2022). *3D-GIS Parametric Modelling for Virtual Urban Simulation Using CityEngine*. Annals of GIS, 28(3), 325–341. https://doi.org/10.1080/19475683.2022.2037019

Bieda, A., Bydłosz, J., Parzych, P., Pukanská, K., & Wójciak, E. (2020). *3D technologies as the future of spatial planning: The example of Krakow. Geomatics and Environmental Engineering*, 14(1), 15–33. https://doi.org/10.7494/geom.2020.14.1.15

Biljecki, F. (2017). *Level of detail in 3D city models* [TU Delft]. https://doi.org/https://doi.org/10.4233/f12931b7-5113-47ef-bfd4-688aae3be248

Biljecki, F., Stoter, J., Ledoux, H., Zlatanova, S., & Çöltekin, A. (2015). *Applications of 3D city models: State of the art review*. ISPRS International Journal of Geo-Information, 4(4), 2842–2889. https://doi.org/10.3390/ijgi4042842

Buyukdemircioglu, M., Kocaman, S., & Isikdag, U. (2018). *Semi-automatic 3D city model generation from large-format aerial images*. Canadian Historical Review, 7(9). https://doi.org/10.3390/ijgi7090339

Danilina, N., Slepnev, M., & Chebotarev, S. (2018). Smart city: Automatic reconstruction of 3D building models to support urban development and planning. *MATEC Web of Conferences, 251*. https://doi.org/10.1051/matecconf/201825103047

Firdaus, Z. M., Handayani, H. H., & Hidayat, H. (2020). *Utilization of LiDAR Data and Aerial Photos for Three-Dimensional City Modeling (Case Study: West Surabaya Region)*. Geoid, 16(1), 80–92.

Foody, G. M. (2002). *Status of land cover classification accuracy assessment.* Remote Sensing of Environment, 80, 185–201. www.elsevier.com/locate/rse

Heipke, C., Mayer, H., Wiedemann, C., & Jamet, O. (1997). Evaluation of Automatic Road Extraction. *International Archives of Photogrammetry and Remote Sensing*, 32, 151–160.

Herbert, G., & Chen, X. (2015). *A comparison of usefulness of 2D and 3D representations of urban planning*. Cartography and Geographic Information Science, 42(1), 22–32. https://doi.org/10.1080/15230406.2014.987694

Jang, Y. J., Oh, J. H., & Lee, C. N. (2020). *Urban Building Change Detection Using nDSM and Road Extraction*. Journal of the Korean Society of Surveying, Geodesy, Photogrammetry and Cartography, 38(3), 237–246.

Kelly, T. (2021). *CityEngine: An Introduction to Rule-Based Modeling. In Urban Book Series* (pp. 637–662). Springer Science and Business Media Deutschland GmbH. https://doi.org/10.1007/978-981-15-8983-6_35

Pađen, I., García-Sánchez, C., & Ledoux, H. (2022). *Towards automatic reconstruction of 3D city models tailored for urban flow simulations*. Frontiers in Built Environment, 8. https://doi.org/10.3389/fbuil.2022.899332

Peraturan Badan Informasi Geospasial Nomor 18 Tahun 2021 Tentang Tata Cara Penyelenggaraan Informasi Geospasial, Badan Informasi Geospasial (2021). https://peraturan.bpk.go.id/Details/217091/peraturan-big-no-18-tahun-2021

Peters, R., Dukai, B., Vitalis, S., van Liempt, J., & Stoter, J. (2022). *Automated 3D Reconstruction of LoD2 and LoD1 Models for All 10 Million Buildings of the Netherlands*. Photogrammetric Engineering and Remote Sensing, 88(3), 165–170. https://doi.org/10.14358/PERS.21-00032R2

Raven, J., Leone, M. F., Mills, G., Katzschner, L., Gaborit, P., Georgescu, M., Hariri, M., & Stone, B. (2018). *Urban planning and urban design. In Climate Change and Cities* (ARC 3-2). Second Assessment Report of the Urban Climate Change Research Network (pp. 139–172). Cambridge Univesity Press.

Trikusuma, F., Prasetyo, Y., & Hadi, F. (2021). Pemodelan 3 (Tiga) *Dimensi Bangunan Menggunakan Foto Udara Format Kecil (Studi Kasus: Fakultas Teknik, Universitas Diponegoro).* Jurnal Geodesi UNDIP, 10(2), 1–10.

Udoh, U. P., Essien, A. U., & Etteh, D. I. (2020). *The Importance of Urban Design and Sustainable Urban Transformation in Nigeria*. IOSR Journal Of Humanities And Social Science (IOSR-JHSS, 25(6). https://doi.org/10.9790/0837-2506060107

Uggla, M., Olsson, P., Abdi, B., Axelsson, B., Calvert, M., Christensen, U., Gardevärn, D., Hirsch, G., Jeansson, E., Kadric, Z., Lord, J., Loreman, A., Persson, A., Setterby, O., Sjöberger, M., Stewart, P., Rudenå, A., Ahlström, A., Bauner, M., … Harrie, L. (2023). Future Swedish 3D City *Models—Specifications, Test Data, and Evaluation*.

ISPRS International Journal of Geo-Information, 12(2). https://doi.org/10.3390/ijgi12020047

Willenborg, B., Sindram, M., & Kolbe, T. H. (2018). *Applications of 3D City Models for a better understanding of the Built Environment*. In M. Behnisch & G. Meinel (Eds.), Trends in Spatial Analysis and Modelling (Vol. 19, pp. 167–191). Springer, Cham. https://doi.org/https://doi.org/10.1007/978-3-319-52522-8_9

Winsemius, S., & Braaten, J. (2024). *Zonal Statistics. In Cloud-Based Remote Sensing with Google Earth Engine* (pp. 463–485). Springer International Publishing. https://doi.org/10.1007/978-3-031-26588-4_24

Zheng, Y., Weng, Q., & Zheng, Y. (2017*). A hybrid approach for three-dimensional building reconstruction in indianapolis from LiDAR data*. Remote Sensing, 9(4). https://doi.org/10.3390/rs9040310